



ELECTROCHEMICAL HYDROGEN STORAGE CHARACTERISTICS OF $Mg_{2-x}C_xNi$ ($x= 0, 0.1, 0.2, 0.5$) ALLOYS PREPARED BY MECHANICAL ALLOYING

Sajad Haghanifar, Saeid Kakooei and Mokhtar Che Ismail

Centre for Corrosion Research, Mechanical Engineering Department, Universiti Teknologi Petronas, Tronoh, Perak, Malaysia

E-Mail: haghanifar.s@gmail.com

ABSTRACT

$Mg_{2-x}C_xNi$ ($x= 0, 0.1, 0.2, 0.5$) type alloys were prepared by mechanical alloying and their electrochemical hydrogen storage characteristics were investigated in 6 M KOH solution. Characterization of the crystal structure of the milled products using X-ray diffractometry exhibited the formation of Mg_2Ni -based nano-crystallites after ~5h for the initial mixture with stoichiometric composition of Mg_2Ni and $Mg_{1.9}C_{0.1}Ni$. However, Mg_2Ni -based nano-crystallites were synthesized after 15 and 20h of milling in the case of $Mg_{1.8}C_{0.2}Ni$ and $Mg_{1.5}C_{0.5}Ni$, respectively. The results show that increasing the carbon content of initial powder mixture decreases the formation kinetics of Mg_2Ni -based nano-crystallites. In addition, increasing milling time resulted in decreasing and increasing the mean crystallite size and lattice strain of Mg_2Ni structure in all milled products. Furthermore, the negative electrode made from $Mg_{1.9}C_{0.1}Ni$ ternary milled product after 30 hour of milling exhibited the highest initial discharge capacity and longest discharge life at all the ball milling durations. This observation was attributed to the formation of the porous unstable $Mg(OH)_2$ layer due to the intercalation of Mg, which have the high rate of solubility in strongly basic solutions, and thus the exposition of the underlying electro catalytically active Ni sites for the sample without carbon addition.

Keywords: Mg_2Ni , carbon, hydrogen absorbing materials, electrochemical properties, nano-crystalline, amorphous, mechanical alloying.

INTRODUCTION

Hydrogen energy is a promising solution for energy problems. Among various methods of using hydrogen treat energy, metal-hydrogen systems are considered to have a prospective future for applications because of their characteristics of reversible absorbing / desorbing of hydrogen under moderate conditions. As a typical metal-hydrogen system, magnesium-based alloy is a promising one for the following reasons: (a) light weight, (b) high storage capacity, (c) the material is abundant and available at low cost. But in spite of all these advantages, its poor hydrating / dehydrating properties prevent it from being used in applications.

Rechargeable Ni-MH battery is a battery with a hydrogen storage alloy as its negative electrode, which is able to absorb and desorb reversibly a large amount of hydrogen at room temperature. Such batteries have less detrimental effect on the environment than conventional nickel cadmium ones. Mg_2Ni intermetallic structure is considered to be possible candidate for the negative electrode material [1]. Nano-crystalline Mg_2Ni powder was achieved using high energy ball milling [2]. It was shown that charge-discharge characteristics of Mg_2Ni intermetallic were markedly enhanced by nano-crystallization and amorphization [3]; this can be kinetically improved using elemental additives substituting either Mg [4] or Ni [5] lattice sites. Noticeable improvement in the discharge capacity of the Mg-based alloys can be obtained if these alloys are synthesized by the mechanical alloying (MA). The grain size of the alloys is reduced down to 50 nm by MA and the discharge capacity can be improved up to 200 mAh g⁻¹ at room temperature [6]. Even this improved value, however, is

still much less than the theoretical discharge capacity of Mg_2Ni phases (1000 mAh g⁻¹).

The life cycle of the Mg-based alloys is also unacceptably poor. The improvement in the electrochemical hydrating/dehydrating performance of the Mg-based alloys in alkaline solutions can also be achieved by the partial replacement of Mg and/or Ni in Mg_2Ni phase [7].

Yuan [8] and Orimo *et al.* [9] investigated the effect of graphite (G) or carbon addition during ball milling of Mg and Ni powder and synthesized amorphous $MgNiC_x$ (x up to 1.31). Imamura *et al.* [10-11] also studied the Mg/G composites as prepared by ball milling Mg powder and graphite in the presence of organic additive and found the synergetic interactions between magnesium and graphite as a result of mechanical grinding with the organic additives. Furthermore, carbon is a very interesting element for hydrogen storage. During recent decades, an intended combination of carbon nanotubes and metal hydrides was expected to have a potential application in the field of hydrogen storage [12-13].

In the present work, carbon powder is used as an additive to elemental powder mixtures of Mg and Ni. Previous investigation showed positive effect of carbon plus niobium additives on the formation kinetic of quaternary $Mg_{1.75}Nb_{0.125}C_{0.125}Ni$ produced by mechanical alloying [14]. Thus, microstructure and electrochemical behaviour of mechanically alloyed powder mixtures of the $Mg_{2-x}C_xNi$ ($x= 0, 0.1, 0.2, 0.5$) type alloys were investigated.



EXPERIMENTAL PROCEDURES

Magnesium tears, Ni and C powders with a purity ~99.5wt. % was used as the starting materials. Ball milling was performed employing a planetary mill equipped with two tempered steel vials containing Cr- steel balls ($\phi=20\text{mm}$). A fixed ball/powder weight ratio and rotation speed of 20:1 and 600rpm were used, respectively. Milling was conducted under argon gas atmosphere for variable times of 5, 15, 30 and 60h. X-ray diffraction patterns of the milled products were obtained using a Cu-K α radiation. The morphology of the milled products was studied using field emission scanning and transmission electron microscopy. The charge/discharge tests were performed at room temperature in 6M KOH solution using a three-electrode cell. Electrochemical measurements of the negative electrode were carried out using a Wonatech WPG100e model potentiostat/galvanostat. The negative electrode was composed of 200mg milled product mixed thoroughly with 800mg of pure nickel powder and 3 drops of 10% polyvinyl alcohol solution to form a paste. The paste was placed around a nickel foam sheet (150×100 mm) and then mechanically pressed to make a compact electrode. The counter electrode and the reference electrode were a nickel plate and a Pt wire, respectively. The negative electrodes were charged at 500mA/g for 5h and discharged at 100mA/g to the cut-off potential of -0.4V versus reference electrode

RESULT AND DISCUSSIONS

Structural and morphological characteristics

Figure-1 shows the XRD patterns of the milled products after different milling time. In according figure 1, it is clear that for case without carbon, Mg_2Ni peaks are appeared in 5 hours. For case $\text{Mg}_{1.9}\text{C}_{0.1}\text{Ni}$, Mg_2Ni peaks have less intensity in 5 hours and for two other cases ((c) $\text{Mg}_{1.8}\text{C}_{0.2}\text{Ni}$ and (d) $\text{Mg}_{1.5}\text{C}_{0.5}\text{Ni}$), Mg_2Ni peaks are not made in the same milling time.

The results show that increasing the carbon content of initial powder mixture decreases the formation kinetics of Mg_2Ni -based nano-crystallites. In the case of binary powder mixture, the milled product was consisted of dominant mixture of Ni, Mg and substantial Mg_2Ni crystal structures. Peaks of Mg_2Ni phase with relative low intensities indicate the beginning of the alloying process. In addition, for the ternary systems with increasing milling time, intensity of peaks has increased. Diffraction peak intensities of Ni showed decreasing by increasing milling times. Also, gradual peak broadening was observed. The peak broadening indicates that the crystallite size decreases rapidly at the beginning of milling and then levels off. Probably, this can be due to an increase in the specific area of the powder and an increase in the number of lattice defects caused by the mechanical milling. Furthermore, XRD results show the formation of an amorphous phase. With further milling, crystallization of amorphous into nano-crystalline Mg_2Ni occurred.

According to Figure-1, sharp diffraction lines of Mg and Ni gradually became broader and their intensities

decreased with milling time. The nanostructured Mg_2Ni related to broad diffraction peaks was found after 30h (Figure-1c and d) and 5h (Figure-1a and b) of milling.

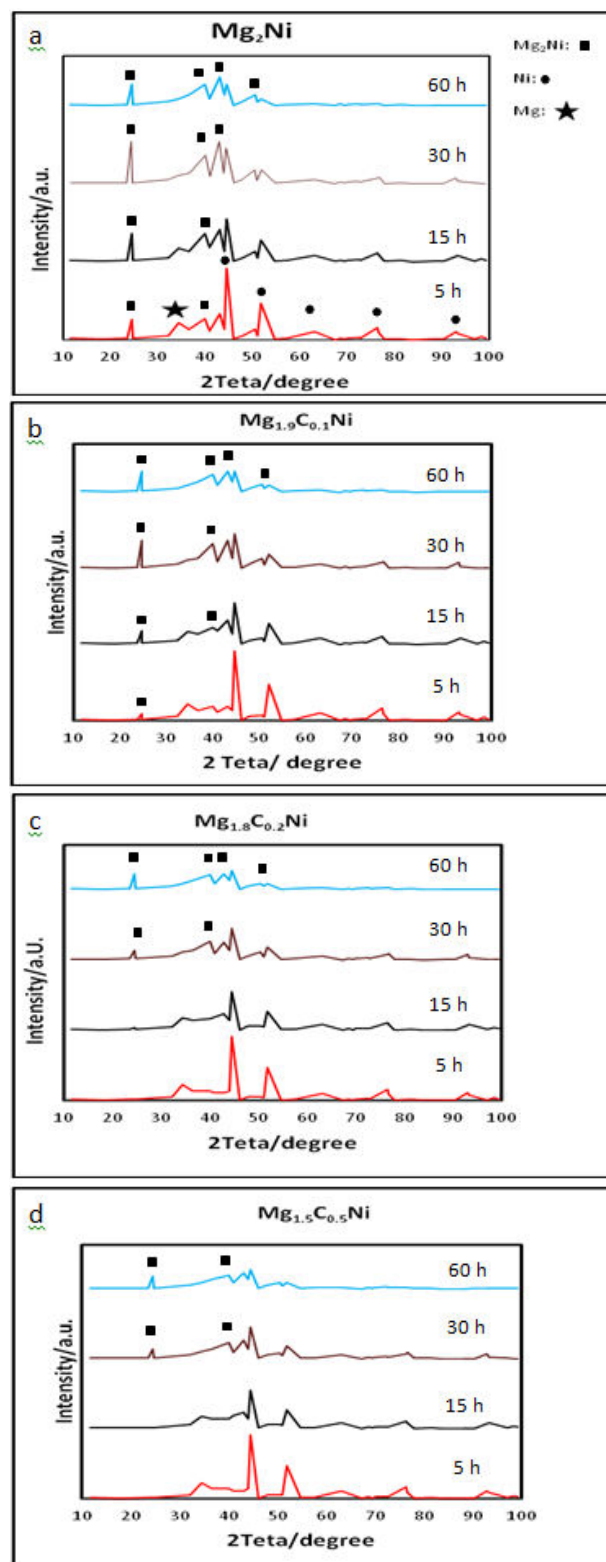


Figure-1. X-ray diffraction pattern of the milled products using the initial powder mixture of Mg_2Ni (a), $\text{Mg}_{1.9}\text{C}_{0.1}\text{Ni}$ (b), $\text{Mg}_{1.8}\text{C}_{0.2}\text{Ni}$ (c) and $\text{Mg}_{1.5}\text{C}_{0.5}\text{Ni}$ (d) as a function of milling time.



The crystallite size and internal strain were calculated from the following equation [6].

$$\beta = \frac{0.9\lambda}{t \cos \theta} + \eta \tan \theta \quad (1)$$

Where β is the peak widths at half maximum intensity of the reflection with highest intensity, λ is the wavelength, θ is the Bragg angle at maximum intensity, t is the average diameter of crystallites (\AA) and η is the lattice strain. The calculated mean crystallite size of Mg_2Ni -based crystallites and their associated lattice strain are shown in Table-1. Increasing milling time is associated with decreasing mean crystallite size and increasing lattice strain.

Several hypotheses have to be considered to explain the origin of the mechanically - induced crystallization of amorphous Mg_2Ni during prolonged milling. One factor which can induce an amorphous to crystalline transformation during ball milling is the temperature increase in the course of milling process. This could be above the crystallization temperature of the amorphous phase. The crystallization temperature of an Mg-Ni alloy into Mg_2Ni crystal structure was determined to be 324°C from differential scanning calorimetric measurements [5]. The actual temperature of individual particle during ball milling can be high enough to cause crystallization.

The mean Mg_2Ni crystallite size of Mg_2Ni , $\text{Mg}_{1.9}\text{C}_{0.1}\text{Ni}$, $\text{Mg}_{1.8}\text{C}_{0.2}\text{Ni}$ and $\text{Mg}_{1.5}\text{C}_{0.5}\text{Ni}$ were calculated to be about 10, 10, 14 and 21 nm after 30h of milling, respectively. The former for $\text{Mg}_{1.9}\text{C}_{0.1}\text{Ni}$ was found to be consistence with transmission electron observation

(Figure-2). This indicates volume expansion of Mg_2Ni -based crystal structure in the case of ternary milled products possibly due to the presence of carbon. A broad diffuse scattering halo was observed after 30h which implies that the ternary milled product ($\text{Mg}_{1.9}\text{C}_{0.1}\text{Ni}$) becomes partially amorphous (Figure-2b).

Scanning electron micrographs of $\text{Mg}_{1.9}\text{C}_{0.1}\text{Ni}$ alloy synthesized by various hour milling are given in Figure-4. SEM observations indicate that particle size decreases with increasing milling time. After milling, the particles were reduced in size, however agglomerated. The fragmentation of the coarse, cold welded particles into the fine powders in Figure-4a and d shows the typical morphology of the amorphous-like alloys [6].

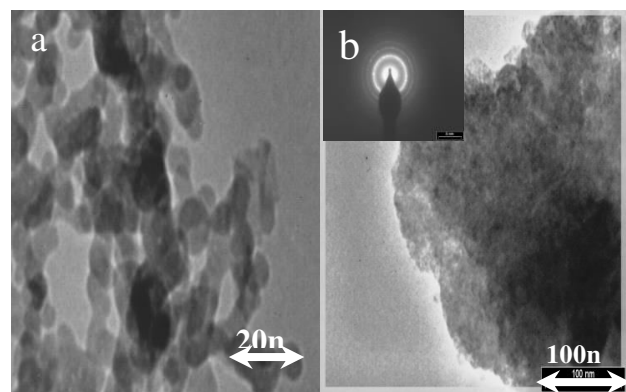


Figure-2. Transmission electron micrograph of the $\text{Mg}_{1.9}\text{C}_{0.1}\text{Ni}$ milled products after 30h.

Table-1. Mean Mg_2Ni crystallite size and its associated lattice strain as a function of milling time.

Milling time (hour)	Mg2Ni mixture		Mg1.9C0.1Ni mixture		Mg1.8C0.2Ni mixture		Mg1.5C0.5Ni mixture	
	Lattice strain[%]	Mean Crystallite size[nm]	Lattice strain[%]	Mean Crystallite size[nm]	Lattice strain[%]	Mean Crystallite size[nm]	Lattice strain[%]	Mean Crystallite size[nm]
7	0.341	40.8	0.273	43.2	0.265	45.1	0.253	47.6
10	0.383	37.6	0.338	38.1	0.294	39.4	0.298	44.2
12	0.592	19.1	0.512	17.3	0.452	33.2	0.459	39.5
20	0.896	10.8	0.746	11.2	0.644	25.6	0.618	34.3
30	0.943	10.1	0.814	10.7	0.751	19.7	0.763	28.9
60	0.971	9.6	0.89	10.01	0.826	14.1	0.812	21.2

3.2 Discharge capacity of the binary and ternary alloys

Figure-4 shows the typical galvanostatic discharge curves of electrodes prepared from the binary and ternary products after 30h of milling in 6M KOH aqueous solution. The discharge voltage curves show that the voltage platforms of ternary electrodes are wider and slightly higher than that of the binary one. Also, a faster potential dropping is found in the binary electrode (C-free)

than the ternary ones. This implies the better performance of the ternary electrodes than C-free one. For galvanostatic method, the discharge capacity of the hydride is determined by two factors. One is the quantity of the active substances that can release hydrogen (i.e. the nanocrystalline or amorphous phase in the hydride), and the other is the electrochemical kinetics of the hydride. The ternary electrodes have more amorphous or nanocrystalline phases and crystal defects, such as



dislocations, grain boundaries, etc. This may be due to the differences of the structural and morphological characteristics. The larger number of interfaces and grain boundaries provide more efficient active sites for charge-transfer reaction. Besides, hydrogen may reach the surface more rapidly for a smaller particle. Therefore, the addition of carbonaceous materials at particular amount significantly improves both the amount of active substance and the electrochemical kinetics, and hence increases the discharge capacity. It is well-known that these carbonaceous materials are important hydrogen storage materials [15]. However, in present case, this small amount of carbon additive can hardly make a contribution to discharge capacity. Thus, the high discharge capacity must come from the amorphous or nanocrystalline Mg_2Ni -based hydride phase.

The initial electrode capacity as a function of milling time is presented in Figure-5. The discharge capacity was found to increase with increasing milling time up to 30h and then decrease for longer times. Obviously the grain refinement and development of the nanocrystalline/amorphous structure increase the hydrogen storage capacity of Mg_2Ni alloy. It is clearly seen that the $\text{Mg}_{1.9}\text{C}_{0.1}\text{Ni}$ electrode fabricated from the 30h milled product has the maximum discharge capacity; this is associated with the presence of finest Mg_2Ni crystallites. But, as the milling time increases, an amorphous phase becomes dominant which is more likely to be related to lowering the discharge capacities. It is believed that the introduction of defects and internal strain can give rise to an increase in hydrating/dehydrating rate and hydrogen capacity. Also, the lower discharge capacity of the milled product with the dominant amorphous microstructure is presumably attributed to its disordered structure. Although more available sites for hydrogen storage are associated with an amorphous phase rather than the crystalline one due to volume expansion, but it is presumed that noncrystalline structure is not able to maintain hydrogen atoms [6].

Nickel is well known to have a high electro catalytic activity or a low over potential for the hydrogen evolution reaction in alkaline solution [5]. The nickel content of the ternary electrodes is more than that of the binary one. It is highly probable that fine nanoscale nickel particles distributed within the ternary milled products. Therefore, these particles can act as the electro catalytic sites for the hydrogen evolution reaction so that the charge transfer resistance is reduced and resulted in a significant increase of electrochemical capacity. At the same time, the decrease of the particle size and the augmentation of the defects density may improve the diffusion of hydrogen in the electrode. This is believed to be beneficial to the reaction kinetics of hydrating/dehydrating. The amount of nickel controls the kinetics of electrochemical reactions, while the heat of hydride formation controls the hydrogen storage capacity and hydrogen absorption/desorption diffusion rate.

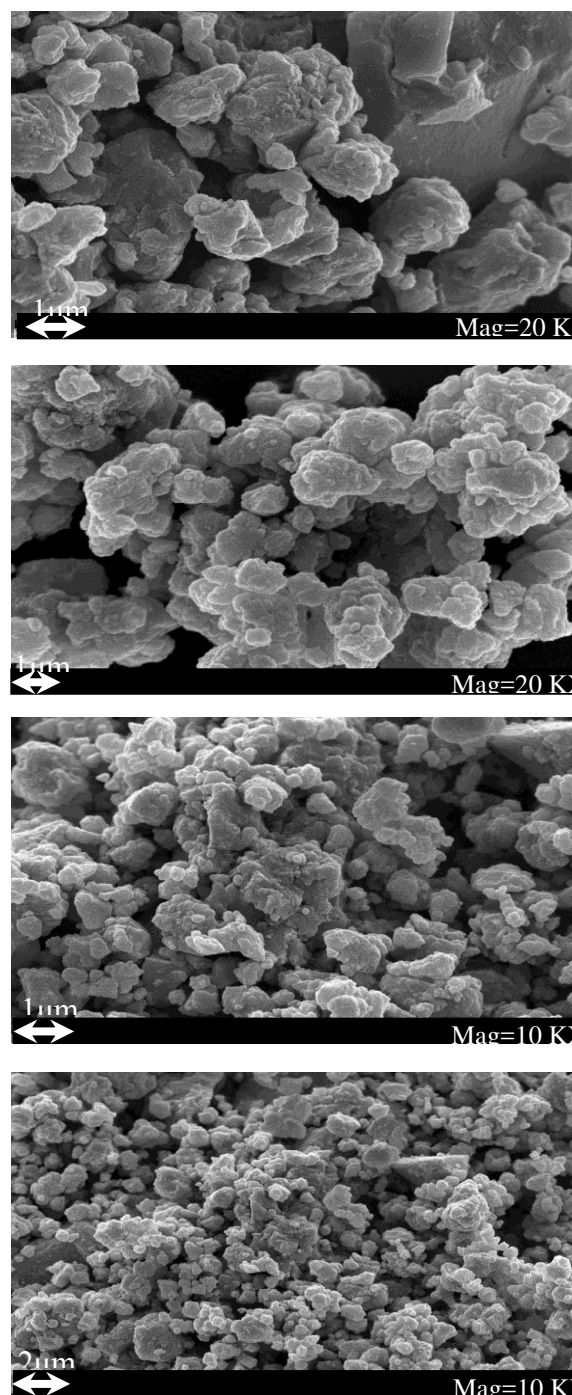


Figure-3. Scanning electron micrograph of the $\text{Mg}_{1.9}\text{C}_{0.1}\text{Ni}$ milled products after 5 hours (a), 15 hours (b), 30 hours (c) and 60 hours (d) of milling time.

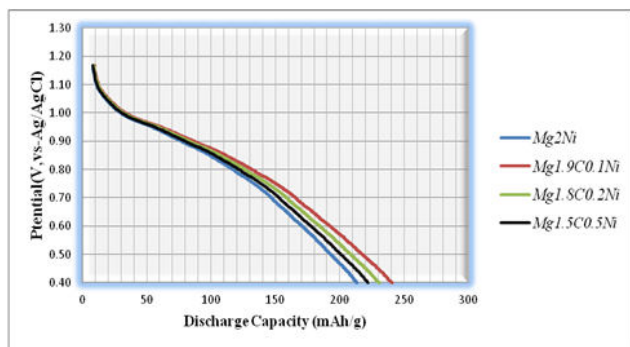


Figure-4. Galvanostatic discharge curves of electrodes prepared from the binary and ternary products after 30h of milling in 6M KOH aqueous solution.

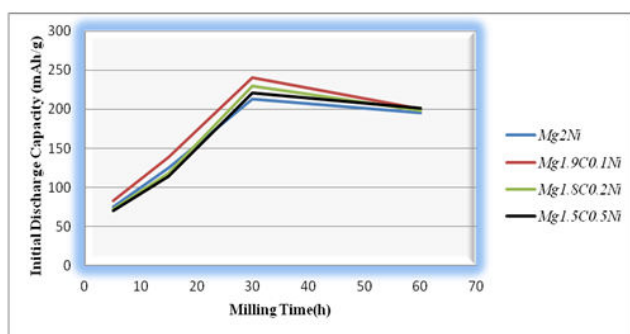


Figure-5. Initial discharge capacity of the milled products as a function of milling time.

CONCLUSIONS

$Mg_{2-x}C_xNi$ ($x = 0, 0.1, 0.2, 0.5$) type alloys were synthesized by mechanical alloying and their electrochemical hydrogen storage characteristics were investigated. The following conclusions may be deduced:

- Small amount substitution of C for Mg was found to accelerate the formation of Mg_2Ni nano-crystallites in mechanical alloying of $Mg_{1.9}C_{0.1}Ni$ powder mixture.
- The electrode fabricated from the ternary $Mg_{1.9}C_{0.1}Ni$ product exhibited an initial discharge capacity of ~241 compared to 213 mAh/g of binary Mg_2Ni .
- The discharge capacity was found to increase with increasing milling time up to 30h and then decrease for longer times.
- The $Mg_{1.9}C_{0.1}Ni$ electrode fabricated from the 30h milled product has the maximum discharge capacity; this is associated with the presence of finest Mg_2Ni crystallites. But, as the milling time increases, an amorphous phase becomes dominant which is more likely to be related to lowering the discharge capacities.
- The C content electrodes prevent the rapid degradation of Mg_2Ni phase with the charge/discharge cycles.

ACKNOWLEDGEMENT

Partial financial support by the Iranian Nanotechnology Initiative Council and University of Tehran is gratefully acknowledged.

REFERENCES

- [1] Y. Zheng, H. Wang, T. Zhai, T. Yang, Z. Yuan, D. Zhao, 2015, Hydrogen storage performances of $LaMg_{11}Ni + x$ wt% Ni ($x = 100, 200$) alloys prepared by mechanical milling, *Journal of Alloys and Compounds*, 645: 438-445.
- [2] A. Ebrahimi-Purkani, S. F. Kashani-Bozorg. 2008. Nanocrystalline Mg_2Ni -based powders produced by high-energy ball milling and subsequent annealing, *Journal of Alloys and Compounds*, 456: 211-215.
- [3] M. Mohri and S. F. Kashani-Bozorg. 2011, Comparison of electrode properties of binary, ternary and quaternary nanocrystalline Mg_2Ni based powders, *International Journal of Nanoscience*, 10(4-5): 1067-1071.
- [4] S. F. Kashani-Bozorg, M. Mohri, A. Ebrahimi-Purkani. 2008, Electrode Properties of Nanostructured and Amorphous $Mg_{1.75}Nb_{0.25}Ni$ Compound Produced by Mechanical Alloying, *Advanced Materials Research*, 55-57: 581-584.
- [5] M. Mohri, S. F. Kashani-Bozorg. 2008. An electrochemical investigation of nanocrystalline $Mg_2Ni_{0.75}Nb_{0.25}$ compound synthesized by mechanical alloying, *International Journal of Modern Physics B*, 22: 2939-2946.
- [6] V. Yu Zadorozhnyy, M. Menjo, M. Yu Zadorozhnyy, S. D. Kaloshkin, D. V. Louzguine-Luzgin, 2014, Hydrogen sorption properties of nanostructured bulk Mg_2Ni intermetallic compound, *Journal of Alloys and Compounds*, 586: 400-404.
- [7] M. Anik, H. Gasan, S. Topcu, I. Akay, N. Aydinbeyli. 2009. Electrochemical hydrogen storage characteristics of $Mg_{1.5}Al_{0.5-x}Zr_xNi$ ($x = 0, 0.1, 0.2, 0.3, 0.4, 0.5$) alloys synthesized by mechanical alloying, *Journal of Hydrogen Energy*, 2009, 34: 2692-2700.
- [8] A. Yuan, N. Xu. 2001, A study on the effect of nickel, cobalt or graphite addition on the electrochemical properties of an AB_5 hydrogen storage alloy and the mechanism of the effects, *Journal of Alloys and Compounds*, 322(1-2): 269-275.
- [9] K. Funaki, S. I. Orimo, H. Fujii, H. Sumida. 1998. Structural and hydriding properties of amorphous $MgNi$ with interstitially dissolved carbon, *Journal of Alloys and Compounds*, 270(1-2): 160-163.



- [10] H. Imamura, S. Tabata, N. Shigetomi, Y. Takesue, Y. Sakata. 2002. Composites for hydrogen storage by mechanical grinding of graphite carbon and magnesium, *Journal of Alloys and Compounds*, 330-332: 579-583.
- [11] H. Imamura, N. Sakasai, T. Fujinaga. 1997, Characterization and hydriding properties of Mg-graphite composites prepared by mechanical grinding as new hydrogen storage materials, *Journal of Alloys and Compounds*, 253-254: 34-37.
- [12] A. Weidenkaff, S.G. Ebbinghaus, Ph. Mauron, A. Reller, Y. Zhang, A. Züttel. 2002. Metal nanoparticles for the production of carbon nanotube composite materials by decomposition of different carbon sources, *Materials Science and Engineering: C*, 19(1-2): 119-123.
- [13] X.P. Gao, X. Qin, F. Wu, H. Liu, Y. Lan, S.S. Fan, H.T. Yuan, D.Y. Song, P.W. Shen. 2000, Synthesis of carbon nanotubes by catalytic decomposition of methane using LaNi₅ hydrogen storage alloy as a catalyst, *Chemical Physics Letters*, 327(5-6): 271-276.
- [14] M. Sharbati and S. F. Kashani-Bozorg. 2012, Evolution of Nano-crystalline Structures using High Energy Ball Milling of Quaternary Mg_{1.75}Nb_{0.125}C_{0.125}Ni and Binary Mg₂Ni, *Acta Physica Polonia A*, 12, 211-213.
- [15] Y. Zhu, W. Zhang, C. Yang, L. Li. 2010, Electrochemical properties of Mg-based hydrogen storage materials modified with carbonaceous materials prepared by hydriding combustion synthesis and subsequent mechanical milling (HCS + MM), *International Journal of Hydrogen Energy*, 35(18): 9653-9660.
- [16] H. Zhen, Z. Wang, H. Zhou, C. Ni, J. Deng, Q. Yao, 2013, Hydrogen storage properties and thermal stability of amorphous Mg₇₀(RE₂₅Ni₇₅)₃₀ alloys, *Journal of Alloys and Compounds*, 563: 1-5.
- [17] Z. P. Guo, Z. G. Huang, K. Konstantinov, H. K. Liu, S.X. Dou. 2006. Electrochemical hydrogen storage properties of nonstoichiometric amorphous MgNi_{1+x}MgNi_{1-x}-carbon composites (x=0.05x=0.05-0.3), *International Journal of Hydrogen Energy*, 31(14): 2032-2039.